Supplementary material: Electrohydrodynamics of particle-covered drops

M. Ouriemi and P. M. Vlahovska

1 Sedimentation effect

Due to the small density difference between the drop and the continuous phase, the drop sediments on the time scale of the experiment (3min). The range of terminal velocities calculated from the balance of Stokes drag and buoyancy forces on a spherical drop is listed in Table 1.

Drop Diameter range	sedimentation velocity range	sedimentation distance
[1 - 5] mm	[0.001 - 0.03] mm/s	[0.2 - 5.5] mm

Table 1: Theoretical estimates of drop sedimentation velocity and the distance travelled over the time of a typical experiment.

The particles at the drop interface also experience buoyancy. Their theoretical terminal velocities are listed in Table 2. Apart from the large aluminum particles ($r = 100\mu m$) and glass spheres ($r = 50\mu m$), the particles velocity ($< 7.10^{-4}$ mm/s) is negligible compared to the drop velocity.

Shape and Type	ρ_p (kg/m^3)	r (μm)	v_p (mm.s)	particles direction
random Aluminum (Al)	2600	1.5, 12, 100	1.10^{-5} 7.10^{-4} 0.5	bottom
spherical Al coated ceramic (Ac)	850	6	1.10^{-5}	up
spherical glass (G)	2200	5, 8.5, 50	1.10^{-4} 3.10^{-4} 0.1	bottom
random fingerprint (F)	2080	0.5	9.10^{-7}	bottom
spherical polyethylene (Pe)	1000	50	3.10^{-4}	bottom
spherical PMMA (P)	1200	8.5	5.10^{-5}	bottom
random silver (Si)	8900	1.5	6.10^{-5}	bottom
spherical Si coated glass (Sg)	2500	8.5	3.10^{-4}	bottom

Table 2: Particles sedimentation velocity (noted v_p).

Figure 1.A illustrates the effect of particle sedimentation after the field is turned off. Most of the particles are initially around the equator forming a belt. The trajectories of some of the particles are shown in Figure 1.B. Particles in both the upper and the lower surface of the drop can be observed, but mainly particles in the lower surface of the drop were recorded. During the measurement ($56s$), particles in the lower part of the drop moved toward the poles while particles in the upper part moved toward the equator. Figure 2 represents the estimated particles velocity (under the assumption of a linear trajectory). The velocity increases when particles go closer to the drop contour in the (y-z plan). Particles localized around the drop contour were not been recorded, but a linear fit of the data, give their mean velocity around $0.015mm/s$. The sedimentation velocity of a silicone drop of radius 2 mm in castor oil is estimated around $0.02mm/s$, while the sedimentation velocity of polyethylene particles is around 3.10^{-4} mm/s. As predicted, the particles motion without electrical fields is mainly due to fluid motion induced by the drop sedimentation. For a drop of radius 2mm, the electrohydrodynamic flow becomes dominant above $Ca \sim 0.2$.

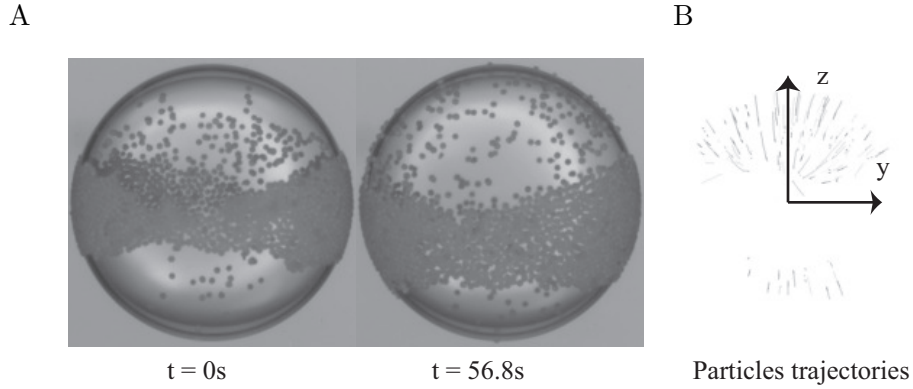

Figure 1: Initial, final state and particles trajectories for a drop covered with polyethylene particles for a surface coverage $\phi = 35\%$ and Ca $= 0$

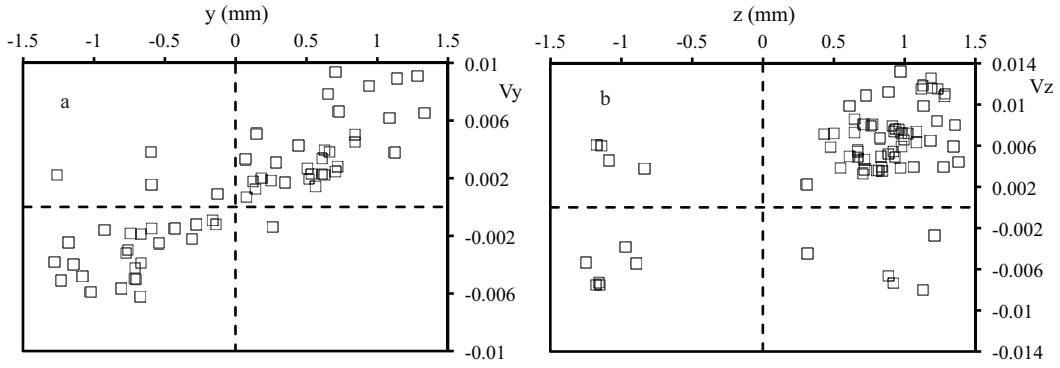

Figure 2: a - y component of the velocity of the particles as a function of their horizontal position. b- z component of the velocity of the particles as a function of their vertical position

2 Belt width

Figure 3 illustrates the effect of field strength on the belt width for drops covered with different types of particles and coverage. A slight decrease of the belt width can be noticed for every type of particles tested suggesting an increase of the compressive stress with the field strength. Ca_S denotes the threshold for belt buckling and formation of a sinusoid, while Ca_o denotes the threshold for drop wobbling/tumbling.

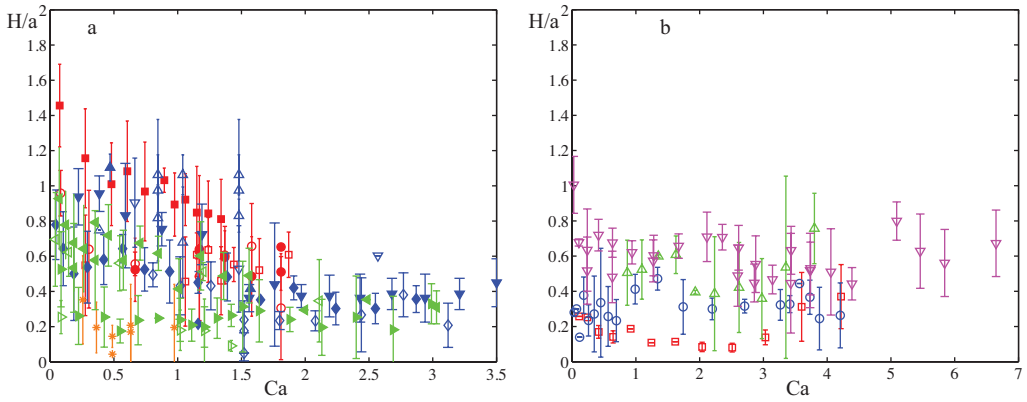

Figure 3: Belt width (normalized by the drop radius a) as a function of the field strength : a- for belts that undergo transition to sinusoid, b- for belts that remain intact but drops undergo tumbling (Al). a- The empty and filled $\square$ symbols correspond to drops covered with Ac with $\varphi = 37\%$ ($Ca_S > 1.25$) and 61% ($Ca_o > 1.10$), the empty and filled $\circ$ symbols correspond to a drop covered with Al ($r = 1.5\mu m$) with $\varphi = 54\%$ ($Ca_S > 1.17$) and 50% ($Ca_S > 1.50$), the symbols $\star$ denote drops covered with F with $\varphi = 15\%$ ($Ca_S > 0.36$), the symbol $\triangle$ denotes drops covered with G ($r = 5\mu m$, $\varphi = 51\%$, $Ca_S > 0.84$). The empty and filled $\diamond$, filled symbol $\triangle$, empty and filled $\triangledown$ symbols correspond to drops covered with G with respectively $\varphi = 38\%$ ($Ca_S > 1.02$), 40% ($Ca_S > 1.16$), 53% ($Ca_S > 0.5$), 58% ($Ca_S > 0.67$) and 59% ($Ca_S > 1.56$). The empty and filled symbol $\triangleright$, the empty and filled $\triangleleft$ symbols correspond to drops covered with Pe with respectively $\varphi = 8\%$ ($Ca_S > 0.09$), 16% ($Ca_S > 1.11$), 28% ($Ca_S > 1.20$), and 34% ($Ca_S > 1$). b - The symbols $\square$, $\circ$, $\triangle$ and $\triangledown$ correspond to drops covered with Al with respectively $\varphi = 1\%$ ($Ca_o > 1.61$), 22% ($Ca_o > 1.74$), 38% and 48% ($Ca_o > 1.67$)

3 Wavelength

Figure 4 shows the wavelength Λ as a function of the belt width H for different types of particles and coverages. The wavelength increases with the belt width H. The strong dependence on H is probably due to the energy cost for bending.

4 Chains regime

Figure 5 shows the evolution of the belt structure and width with increasing fields strength for highly conductive spheres (Si) and large low conductivity sphere (G). Unlike the belt formed by low-polarizability particles, particle chaining causes increase of the belt width with the electric field strength. This effect is known as the "pupil-effect".

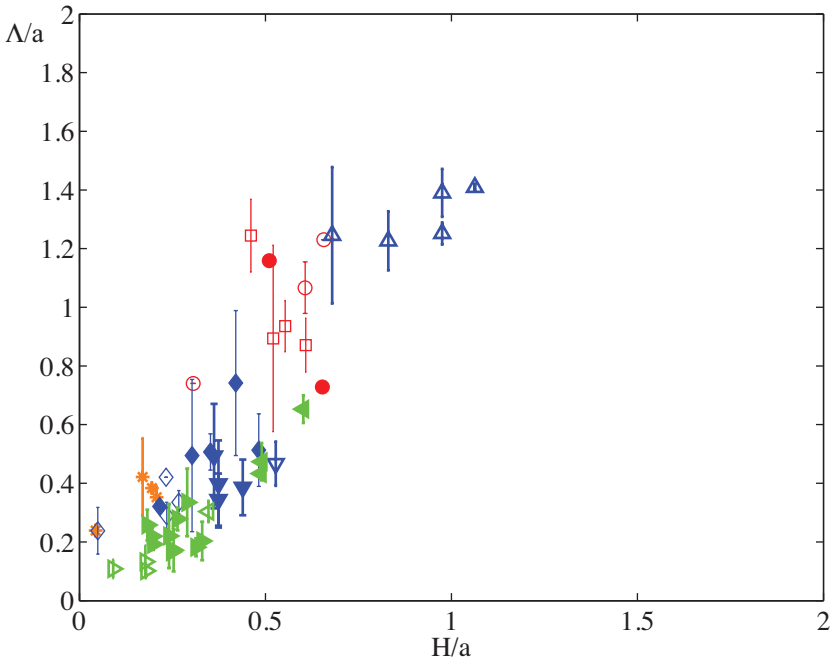

Figure 4: Wavelength Λ as a function of the belt width H (both normalized by the drop radius a). The $\square$ empty and filled symbols correspond to Ac-covered-drops with $\varphi = 37\%$ and 61%, respectively. The empty and filled $\circ$ symbols correspond to a Al-($r = 1.5\mu m$)- covered drop with $\varphi = 54\%$ and 50%, the symbols $\star$ to drops covered with F with $\varphi = 15\%$, the symbol $\triangle$ to drops covered with G ($r = 5\mu m$, $\varphi = 51\%$). G- ($r = 8.5\mu m$)-covered drops with $\varphi = 38\%$, 40%, 53%, 58% and 59% are represented by empty and filled $\diamond$ symbols, the filled symbol $\triangle$, the empty and filled symbols $\bigtriangledown$. The the empty and filled $\triangleright$ symbol, the empty and filled $\triangleleft$ denote Pe-covered drops with $\varphi = 8\%$, 16%, 28% and 34%.

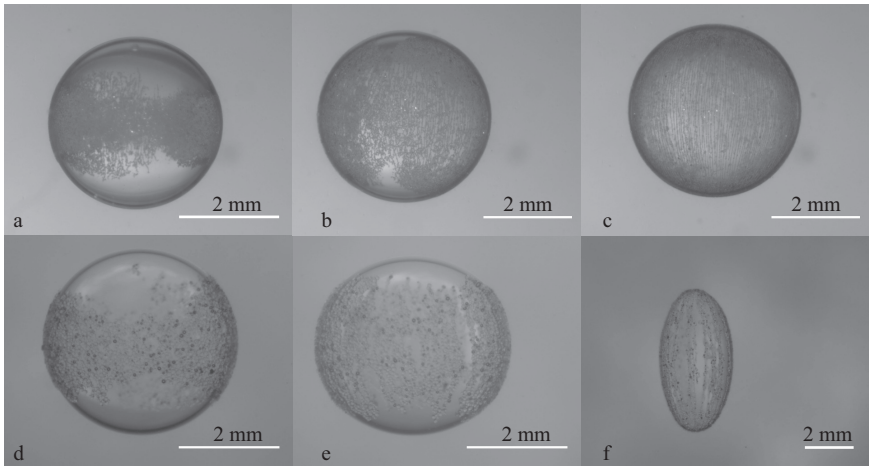

Figure 5: "Pupil like" effect observed for a drop covered with silver coated glass sphere (a to c) and large ($d = 100\mu m$) glass spheres (d to f). a corresponds to $E_0 = 58.6\ kV/m$, b to $E_0 = 71.6\ kV/m$, c to $E_0 = 111\ kV/m$, d to $E_0 = 61.6\ kV/m$, e to $E_0 = 175\ kV/m$ and f to $E_0 = 345\ kV/m$.